 doi:10.20944/preprints202209.0228.v1

Article

Resting-State Functional Connectivity Impairment in Patients with the Major Depressive Episode

Drozdstoy Stoyanov [1], Vladimir Khorev [2,3], Rossitsa Paunova [1], Sevdalina Kandilarova [1], Denitsa Simeonova [1], Artem Badarin [2,3,4], Alexander Hramov [2,3,4] and Semen Kurkin [2,3,4]

[1] Department of Psychiatry and Medical Psychology, Research Institute, Medical University Plovdiv, 4002 Plovdiv, Bulgaria
[2] Baltic Center for Artificial Intelligence and Neurotechnology, Immanuel Kant Baltic Federal University, Russia
[3] Neuroscience and Cognitive Technology Laboratory, Innopolis University, Russia
[4] Neuroscience Research Institute, Samara State Medical University, Russia

Abstract: Aim. In the current study, we aimed at identifying resting-state brain networks, which are different in patients with depression compared to healthy individuals. Moreover, we analyzed the potential for clinical use of different network measures that could discriminate the two groups and thus help the diagnostic process. Method and subjects. We recruited 90 subjects: 49 healthy controls (HC) and 41 patients with a major depressive episode (MDE). All subjects underwent clinical evaluation and functional resting-state MRI. The data were processed to investigate functional connectivity network measures across the two groups using Brain Connectivity Toolbox. The statistical inferences were made at the functional networks level, using false discovery rate method. Independent samples t-test was performed on the network measures mean values to reveal differences between HC and MDE groups. Permutation-based statistical testing was used to test the significance of the difference between the distributions of the network measures by nodes for HC and MDE groups. Linear discriminant analysis was used to differentiate between the groups. **Results** and discussion. Significant differences in FC between depressed patients and healthy controls were found with the most prominent changes encompassing within-region as well as between-region connectivity of occipital lobe areas such as precuneus (PreCu), cuneus (Cu), superior occipital gyrus (SOG), lingual gyrus (LG), fusiform gyrus (FG), cerebellum, along with limbic structures including the hippocampus (Hipp) and cingulate gyrus. Linear discriminant analysis demonstrated that the full connectivity matrices, as well as those with only the significant connections identified in advance, were the most precise in differentiating between depression and health. These measures reached precision levels of 97% and 94%, respectively. Conclusion. Our study delivered further evidence about impairment of functional connectivity networks in MDE that may contribute to differentiate patients with depression from healthy subjects.

Keywords: functional connectivity; functional magnetic-resonance imaging; resting state; mood disorders; classification

1. Introduction

Major depressive disorder (MDD) is a leading cause of disability worldwide (1). However, its exact pathophysiological mechanisms remain unclear. Symptoms of depressive episode include sadness, anhedonia, insomnia, restlessness, and suicidal thoughts (2). Moreover, this condition is characterized by impairments in cognitive and emotional processing (3). There is evidence suggesting that cognitive dysfunction could be seen not only in the acute phase but in remission as well, and it could even worsen the condition's outcome (4,5).

Brain networks can be defined as a set of regions that exhibit correlated activity in resting-state condition or during task performance (6, 7). In recent studies, researchers concentrated on building brain functional networks, as well as searching for abnormal

 doi:10.20944/preprints202209.0228.v1

communication between them in order to explain the pathophysiological mechanisms of MDD (8

Resting state networks are frequently used methodology for identifying different brain constructs based on their correlated activity over time, against a region of interest – ROI analysis, seed-based analysis etc. or independent component analysis (ICA) where the independent components are extracted from the BOLD time-series and then are interpret as networks (9). However, for each of those methods there are weaknesses and strengths which is related to the diversity of brain networks differentiating different psychiatric diagnoses (10,11).

Moreover, significant efforts are devoted to the exploration of the neurobiological basis supporting emotion processing and mood regulation which are affected in patients with depressive disorder (12). An increasing number of studies are aiming at explaining brain abnormalities in depressive disorders by means of structural and functional magnetic resonance imaging (MRI) (13). As a result, many different brain regions were reported to be involved in the pathogenesis of depression including most often limbic structures such as the hippocampus (Hipp) and amygdala (Amy). According to a recent study by Yao Z et al., their volume appear to be smaller in depressed patients compared to healthy controls (14).. Other brain regions including hypothalamus, prefrontal cortex, and basal ganglia are known to be related to the Amy and Hipp. In addition, they form a neural functional network of mood regulation (15,16).

Generally, the brain networks which are taught to be involved in depression are the default mode network (DMN), salience network (SN), and executive control network (ECN) (17,18,19). The rostral medial prefrontal cortex (rmPFC) is a key node in the DMN and was reported to support sociocognitive and socio-affective processes which are impaired in patients with major depressive disorder (20). Moreover, decreased thalamic connectivity with the SN was reported in patients with major depressive disorder (17). However, other brain regions are affected by the major depressive disorder as well. Patients with MDD had increased connectivity between the right anterior hippocampus (rAHipp) and lingual gyrus (LinG) (21). In addition, there was also a decreased connectivity between the right posterior hippocampus (rPHipp) and right inferior frontal gyrus (rIFG) (21). On the other hand, decreased connections between the frontoparietal network and subcortical network and increased connections between the frontoparietal network and salience network were reported, which shows the dysregulated neuronal activity in patients with MDD (22).

Understanding brain network dysfunctions in depressionis a promising key in the process of revealing its' pathophysiological mechanism. Previous studies used amplitude of low-frequency fluctuations and resting-state fMRI data in order to observe the connections between DMN and CEN (23). A large study by Liang et al. managed to divide two subgroups of MDD according to their hyper and hypo DMN connectivity (24). They proposed that the hypo-DMN function relates to the age-related severity of depressive symptoms. Bhaskar Sen et al. proposed a different methodology for predicting the chance of suffering from depression by examining connectivity values of brain regions during resting-state fMRI (25). Also, a multivariate approach has been implemented to differentiate MDD and healthy controls where not only cross-network connections were found but also the supramarginal gyrus appeared to be the most discriminative one (26).

There are reported also studies which suggests other regions as significant in terms of classifying MDD. For example, the cognitive control network (CCN) is said to be involved in working memory, decision making, complex cognitive task. However, there are few studies which explicit its functions in MDD patients (27). Moreover, some researches are indicating the affective network as a relevant brain construct in patients with MDD (28).

In the current study, we implemented a new method with which we can contribute to the better understanding of the mechanisms of depression. We aimed at identifying new resting-state brain networks, which are different in patients with MDD compared to healthy individuals. Our goal was to characterize these networks by statistical approaches

Preprints (www.preprints.org) | NOT PEER-REVIEWED | Posted: 15 September 2022 doi:10.20944/preprints202209.0228.v1

and measures such as clustering coefficient, node centrality, and node strength, which address network generative principles, order dependencies, and community structure of networks. Moreover, we analyzed the potential for clinical use of these network characteristics that could discriminate the two groups and thus aid the diagnostic process.

2. Subjects and Methods

2.1. Subjects

We recruited 90 subjects: 49 healthy controls (HC) and 41 patients with a major depressive episode (MDE) in the context of major depressive disorder (n=35) or bipolar affective disorder (n=6). Subjects from both groups were assessed by experienced psychiatrists using Mini International Neuropsychiatric interview (29) and Montgomery–Åsberg Depression Rating Scale (MADRS) (30). Subjects having a previous history of comorbid (for HC and patients, respectively) psychiatric conditions, autoimmune diseases, neurological diseases, history of head trauma, or any metal implants incompatible with the MRI were excluded. All participants provided a written consent form complying with the Declaration of Helsinki. The study was approved by the Medical University of Plovdiv Ethical Committee (Protocol 2/19.04.2018).

Demographic and Clinical Characteristics

The two groups of subjects did not differ significantly in terms of mean age, sex, and level of education distributions. Expectedly, patients had significantly higher MADRS scores (see Table 1).

Table 1. Demographic and clinical characteristics of the groups.

	Healthy controls (n=49)	Patients (n=41)	Statistic	Significance
Age (mean ±SD)	40.7 ± 13.5	41.2 ± 15.4	D-statistic = 0.121	0.842[a]
Sex (M/F)	14/35	14/27	χ^2 - statistic = 0.324	0.569[b]
Education (secondary/higher)	16/33	20/21	χ^2 - statistic = 2.419	0.120[b]
MADRS score (mean ±SD)	2.2 ± 2.9	29.8 ± 8.2	D-statistic = 0.975	$*10^{-22}$ [a]

SD – Standard Deviation, [a] Two-sample Kolmogorov-Smirnov nonparametric test, [b] χ^2 - test, MADRS - Montgomery–Åsberg Depression Rating Scale, * $p<0.05$.

2.2. Methods

2.2.1. MR Scanning

The MR scanning procedure was performed on a 3T MRI system (GE Discovery 750w). The protocol included a high-resolution structural scan (Sag 3D T1) with slice thickness of 1 mm, matrix 256x256, TR (relaxation time) 7.2s, TE (echo time) 2.3 s, and flip angle 12°, FOV 24, 368 slices and resting-state functional scan - 2D echo-planar imaging (EPI), with slice thickness 3 mm, matrix 64 × 64, TR 2000 ms, TE 30 ms, 36 slices, flip angle 90°, FOV 24, a total of 192 volumes. Before the EPI sequence, subjects were instructed to remain as still as possible with their eyes closed and not to think of anything in particular.

2.2.2. Image Processing

Neuroimaging data were processed using SPM 12 software (Statistical Parametric Mapping, http://www.fil.ion.ucl.ac.uk/spm/) running on MATLAB R2021 for Windows. The functional images of each participant were first realigned, co-registered with the high-resolution anatomical image, and normalized to standard MNI space. Parameters for the realignment step were the following: quality 0.9, separation 4, smoothing FWHM 5, 2-nd degree B-spline interpolation, no wrap, 12×12 basis function, regularization 1 with medium factor, without Jacobian deformations, 5 iterations, average Taylor expansion point. The co-registration method was set to the normalized mutual information with the following parameters: separation [4 2], tolerances [0.02 0.02 0.02 0.001

Preprints (www.preprints.org) | NOT PEER-REVIEWED | Posted: 15 September 2022 doi:10.20944/preprints202209.0228.v1

0.001 0.001 0.01 0.01 0.01 0.001 0.001 0.001], histogram smoothing [7 7]. MNI normalization parameters were the following: bias regularization 0.0001, bias FWHM 60mm cutoff, affine regularization ICBM European brain template, warping regularization [0 0.001 0.5 0.05 0.2], no smoothing, sampling distance 3.

2.2.3. Connectivity Matrix Calculation

The normalized functional MRI volumes extracted with the help of SPM12 and the "spm_data_read" function were parcellated into 166 regions according to the automated anatomical labeling atlas AAL3 (31). We have chosen the AAL atlas because it is the most commonly used parcellation scheme in functional network studies (32). To estimate the connectivity between the regions of interest, we calculated an average BOLD time series $x_i(t)$ (across the voxels in each parcellation i) and Pearson correlation coefficients for all pairs of the mean parcellation activities. The Pearson correlation coefficient measures the linear relationship between two random variables and is good for low-frequency processes, which also include fMRI [33. Connectivity Matrix calculation from the averaged activity time series was performed with the help of Matlab statistics "corrcoef" function. Thus, we obtained for each subject a 166×166 symmetric connectivity matrix R. Each cell of the connectivity matrix ($r_{i,j}$) represents the strength of the connection (or edge) between two parcels:

$$r_{i,j} = \frac{\sum_{k=1}^{n}(x_{i,k} - \bar{x}_i)(x_{j,k} - \bar{x}_j)}{\sqrt{\sum_{k=1}^{n}(x_{i,k} - \bar{x}_i)^2}\sqrt{\sum_{k=1}^{n}(x_{j,k} - \bar{x}_j)^2}} \quad (1)$$

Here n is the length of the x time series, and $\bar{x}$ is the mean of the x time series.

2.2.4. Network Measures

To characterize the identified brain networks with meaningful and easily computable indicators, we used the following measures implemented in Brain Connectivity Toolbox (34,35):

1) The weighted undirected clustering coefficient (36), which is typically used as a measure of the prevalence of node clusters in a network. For the particular node i local undirected clustering coefficient of the network can be calculated as follows:

$$C_{clust,i} = \frac{1}{l_i(l_i - 1)} r_{i,j} r_{j,k} r_{k,i},\ i, j, k \in [1..166] \quad (2)$$

where $l_i = \sum_{j=1}^{166} r_{i,j}$ is the total weight of the relationship of the i-th node, 166 is the number of regions. The mean value for the whole network will be:

$$< C_{clust} >= \sum_i C_{clust,i} \quad (3)$$

2) The weighted undirected eigenvector centrality (37), which measures a node's importance while considering the importance of its neighbors. This measure is defined as the eigenvector, v, associated with the largest eigenvalue λ of the correlation matrix, and can be written as:

$$\theta_i = \frac{1}{\lambda_i} \sum_{j=1}^{166} r_{i,j} v_j \quad (4)$$

Preprints (www.preprints.org) | NOT PEER-REVIEWED | Posted: 15 September 2022 doi:10.20944/preprints202209.0228.v1

In analogy with (3), the mean centrality for the network will be denoted as <θ>.

3) The node strength (34), which is the measure representing the sum of the edge weights:

$$Ns_i = \sum_{j=1}^{166} r_{i,j} \quad (5)$$

In analogy with (3), the mean node strength for the network will be denoted as <Ns>.

These measures address network generative principles, order dependencies, and community structure of networks, and they are implemented as a diagnostic tool for explicitly linking micro-scale features of network organization to macro-scale characteristics of neurophysiological dynamics (35).

2.3. Statistical Analysis

Statistical analysis of the demographic and clinical characteristics of the participants was performed using IBM SPSS 28.0 for Windows. The significance level was set to $p < 0.05$. We employed the Chi-square test for the categorical variables (sex and education). We tested the normality of the distributions of the continuous variables with the Kolmogorov-Smirnov one-sample criterion, which did not verify the normality for age and MADRS scores. In that regard, we employed the two-sample Kolmogorov-Smirnov non-parametric test to assess the differences between the control and patient groups.

The false discovery rate (FDR) method (38) with t-test implemented in NBS software (39) was used to assess the differences between the obtained correlation matrices for the two groups (control vs patients) with a significance level of p=0.0001 and 100 000 permutations. We included diagnoses as dummy-coded covariates in the t-test to control the presence of two depressive subgroups (MDD and bipolar).

Independent samples t-test was performed on the network mean values <C_{clust}>, <θ>, <Ns>. Obtained network measures were tested for being normally distributed with the Kolmogorov-Smirnov one-sample criterion.

We applied permutation-based statistical testing (40) to test the significance of the difference (control vs. patients) between the distributions of the network measures by nodes. We revealed the node clusters, which are significantly different between healthy controls and depression groups based on their local values of $C_{clust,i}$, θ_i, Ns_i. Order in the procedure is defined by the neighborhood of the anatomical parcellations, this allows us to analyze the spatial structure of the obtained clusters. For the visualization of the network structures, we used the BrainNet Viewer (41).

2.3.1. Linear Discriminant Analysis

To evaluate the diagnostic value of the identified differences in functional networks between the groups, we applied a linear discriminant analysis (LDA) (in Classification Learner toolbox, Matlab) to data feature vectors from the control and depression groups. Linear discriminant analysis is widely used for diagnostics purposes multivariate supervised classification method to sort objects of study into groups by finding linear combinations of a number of variables [42. The tested variants of feature vectors included: full functional connectivity (FC) matrices, FC matrices with only connections that were considered significant through the FDR analysis, node clustering coefficients, node strength, and node centrality. Statistical significance of the results was ensured by the use of and k-fold (k = 10) cross-validation with each test run 100 times. Names of classes used in the algorithm for training and classification were specified as a categorical set including "control" and "depression". Cost of misclassification of a point was set to the default Cost(i,j)=1 if i≠j, and Cost(i,j)=0 if i=j. A linear coefficient threshold was set to zero. The discriminant type was set to the recommended by the toolbox "pseudolinear" type to avoid problems with zeroes and negative values in the predictors set. Other parameters

Preprints (www.preprints.org) | NOT PEER-REVIEWED | Posted: 15 September 2022 doi:10.20944/preprints202209.0228.v1

including the enforced amount of regularization or prior probabilities were not applied. The chance level of the LDA for the considered problem is 50%.

3. Results

3.1. Connectivity Analysis

Our analysis identified a total of 2673 connections and 152 nodes, which were significantly stronger in the control group compared to the depression group. We present the top 30 of those connections in Table 2 and in Fig. 1.

Table 2. The top 30 significant connections being stronger in the control group compared to the depression group.

	Connection			**Connectivity t-statistic**
1	Precuneus_L	—	Precuneus_R	31,3
2	Cuneus_L	—	Cuneus_R	28,6
3	Cerebellum_4_5_L	—	Cerebellum_4_5_R	28,3
4	Cuneus_R	—	Occipital_Sup_R	24,7
5	Cuneus_L	—	Occipital_Sup_L	24,2
6	Cerebellum_4_5_L	—	Vermis_4_5	21,0
7	Cerebellum_6_L	—	Cerebellum_6_R	20,9
8	Calcarine_R	—	Cuneus_R	20,8
9	Cuneus_R	—	Occipital_Sup_L	20,7
10	Hippocampus_L	—	Hippocampus_R	19,1
11	Calcarine_R	—	Cuneus_L	18,0
12	Cerebellum_4_5_L	—	Cerebellum_6_L	17,3
13	Calcarine_R	—	Occipital_Mid_R	16,7
14	Caudate_L	—	Caudate_R	16,6
15	Cerebellum_3_R	—	Cerebellum_4_5_R	16,5
16	Fusiform_R	—	Cerebellum_4_5_L	16,5
17	Cerebellum_4_5_R	—	Vermis_4_5	16,3
18	Fusiform_R	—	Vermis_4_5	16,3
19	Cingulate_Mid_L	—	Cingulate_Mid_R	16,0
20	Occipital_Sup_R	—	Occipital_Mid_L	15,8
21	Hippocampus_R	—	Temporal_Mid_R	15,5
22	Cuneus_R	—	Occipital_Mid_L	15,2
23	Lingual_L	—	Lingual_R	15,2
24	Hippocampus_L	—	Cerebellum_4_5_L	14,5
25	Fusiform_R	—	Cerebellum_4_5_R	14,4
26	Cerebellum_4_5_R	—	Cerebellum_6_L	14,3
27	Thal_MDm_L	—	Thal_MDl_L	14,2
28	Cerebellum_4_5_R	—	Cerebellum_6_R	13,8
29	Fusiform_R	—	Cerebellum_6_L	13,8
30	Calcarine_L	—	Calcarine_R	13,6

Preprints (www.preprints.org) | NOT PEER-REVIEWED | Posted: 15 September 2022 doi:10.20944/preprints202209.0228.v1

Figure 1. Illustration of the top 30 significant connections being stronger in the control group compared to the depression group.

3.2. Network Analysis

The Kolmogorov-Smirnov one-sample criterion confirmed the normality of the mean network measures processed with the t-test. Mean values for the node strength <Ns> ($t_{2,40}$= 0.179; p=0.8584), node eigenvector centrality <θ> ($t_{2,40}$= 0.004; p=0.9993), and the clustering coefficient <C_{clust}> ($t_{2,40}$= 0.398; p=0.5351) did not show significant difference between the two groups.

Permutation-based statistical testing revealed 5 positive and 2 negative clusters of nodes in the distribution of node eigenvector centrality, 4 positive and 1 negative clusters in the distribution of node strength, and 2 positive and 1 negative clusters in the distribution of clustering coefficient (see Tables 3–5). A positive cluster corresponds to a set of neighboring nodes in which the corresponding network measure is significantly higher in the control group, while for a negative cluster, the network measure is significantly higher in the MDD group.

To construct specific networks, we considered only nodes included in significant clusters (separately for positive and negative ones) and only significant connections between such nodes that were found in the previous step with FDR method. Specific networks for the significant positive clusters for all considered network measures are presented in a unified manner in Fig. 2, and the specific networks for negative clusters are shown in Fig. 3; Tables A1 and A2 in the Appendix contain information about all connections belonging to these networks. The first two positive clusters are very similar for all network measures considered, the 2nd and 3rd are for eigenvector centrality and node strength, and the 5th is unique for eigenvector centrality. The first negative cluster is similar for all network measures considered, and the 2nd is unique for eigenvector centrality.

Preprints (www.preprints.org) | NOT PEER-REVIEWED | Posted: 15 September 2022 doi:10.20944/preprints202209.0228.v1

For the condition Control > MDD, the main hubs common for the considered network measures are the lingual gyrus, the superior occipital gyrus, and the middle occipital gyrus.

Table 3. Significant clusters for the node eigenvector centrality measure; here, superscripts "+" and "-" denote positive and negative clusters, respectively.

Cluster	Nodes	Region	p
1^{+}	49	Lingual L	0.001
	50	Lingual R	
	51	Occipital Sup L	
	52	Occipital Sup R	
	53	Occipital Mid L	
	54	Occipital Mid R	
2^{+}	109	Vermis 1 2	0.005
	110	Vermis 3	
	111	Vermis 4 5	
	112	Vermis 6	
	113	Vermis 7	
3^{+}	35	Cingulate Mid L	0.009
	36	Cingulate Mid R	
	37	Cingulate Post L	
4^{+}	118	Thal AV R	0.014
	119	Thal LP L	
	120	Thal LP R	
5^{+}	7	Frontal Inf Oper L	0.022
	8	Frontal Inf Oper R	
	9	Frontal Inf Tri L	
1^{-}	21	Frontal Med Orb L	0.001
	22	Frontal Med Orb R	
	23	Rectus L	
	24	Rectus R	
	25	OFCmed L	
	26	OFCmed R	
	27	OFCant L	
	28	OFCant R	
2^{-}	121	Thal VA L	0.006
	122	Thal VA R	
	123	Thal VL L	
	124	Thal VL R	

Preprints (www.preprints.org) | NOT PEER-REVIEWED | Posted: 15 September 2022 doi:10.20944/preprints202209.0228.v1

Table 4. Significant clusters for the node strength measure; here, superscripts "+" and "-" denote positive and negative clusters, respectively.

Cluster	Nodes	Region	p
1^{+}	47	Cuneus L	0.005
	48	Cuneus R	
	49	Lingual L	
	50	Lingual R	
	51	Occipital Sup L	
	52	Occipital Sup R	
	53	Occipital Mid L	
2^{+}	109	Vermis 1 2	0.029
	110	Vermis 3	
	111	Vermis 4 5	
	112	Vermis 6	
	113	Vermis 7	
3^{+}	35	Cingulate Mid L	0.050
	36	Cingulate Mid R	
	37	Cingulate Post L	
4^{+}	118	Thal AV R	0.050
	119	Thal LP L	
	120	Thal LP R	
1^{-}	21	Frontal Med Orb L	0.003
	22	Frontal Med Orb R	
	23	Rectus L	
	24	Rectus R	
	25	OFCmed L	
	26	OFCmed R	
	27	OFCant L	
	28	OFCant R	

Preprints (www.preprints.org) | NOT PEER-REVIEWED | Posted: 15 September 2022 doi:10.20944/preprints202209.0228.v1

Table 5. Significant clusters for the clustering coefficient measure; here, superscripts "+" and "-" denote positive and negative clusters, respectively.

Cluster	Nodes	Region	p
1^+	47	Cuneus L	0.009
	48	Cuneus R	
	49	Lingual L	
	50	Lingual R	
	51	Occipital Sup L	
	52	Occipital Sup R	
	53	Occipital Mid L	
2^+	109	Vermis 1 2	0.035
	110	Vermis 3	
	111	Vermis 4 5	
	112	Vermis 6	
	113	Vermis 7	
1^-	21	Frontal Med Orb L	0.003
	22	Frontal Med Orb R	
	23	Rectus L	
	24	Rectus R	
	25	OFCmed L	
	26	OFCmed R	
	27	OFCant L	
	28	OFCant R	

Moreover, Clusters 2–4 are common for the node centrality and node strength indicators.

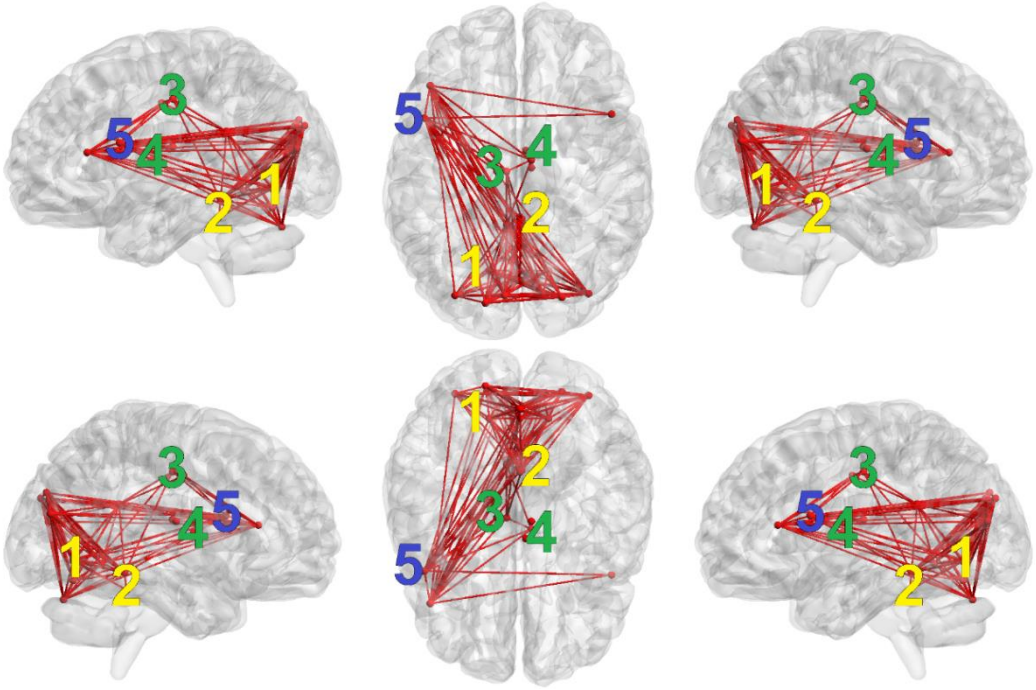

Figure 2. Connected graph obtained for the significant positive clusters (Control > MDD) of the considered network measures. Red dots correspond to the nodes of the clusters, and red lines correspond to the significant connections between the nodes. Numbers denote approximate positions of the clusters (see Table 3). Yellow clusters are similar for all considered network measures, green clusters are similar for eigenvector centrality and node strength, and the blue cluster is unique for eigenvector centrality.

Preprints (www.preprints.org) | NOT PEER-REVIEWED | Posted: 15 September 2022 doi:10.20944/preprints202209.0228.v1

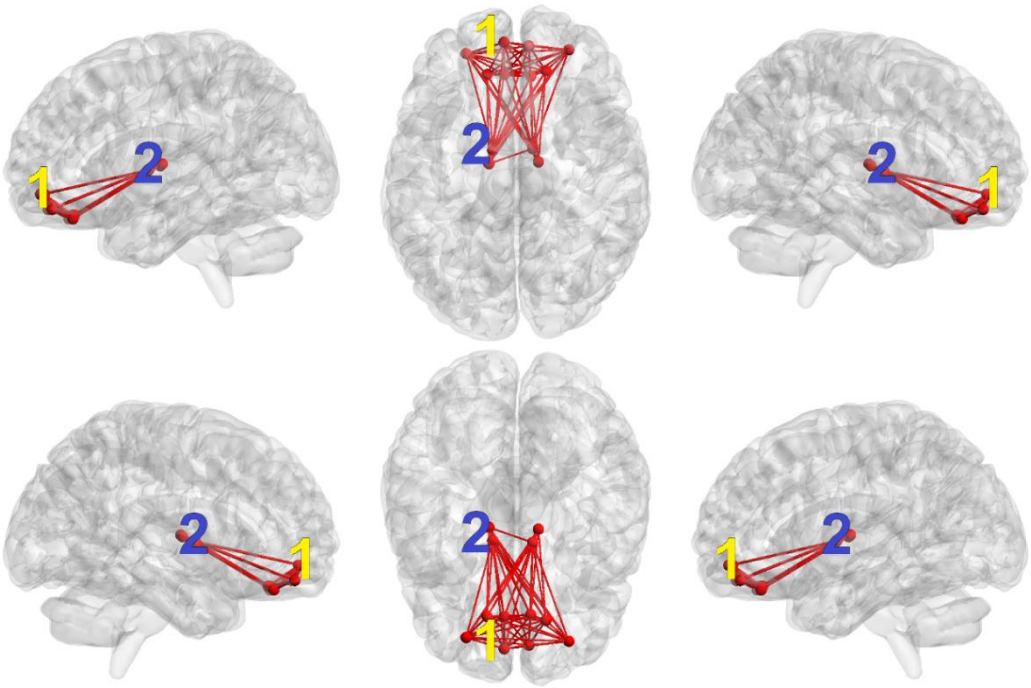

Figure 3. Connected graph obtained for the significant negative clusters (MDD > Control) of the considered network measures. Red dots correspond to the nodes of the clusters, and red lines correspond to the significant connections between the nodes. Numbers denote approximate positions of the clusters (see Table 3). Yellow clusters are similar for all considered network measures, and the blue cluster is unique for eigenvector centrality.

Preprints (www.preprints.org) | NOT PEER-REVIEWED | Posted: 15 September 2022 doi:10.20944/preprints202209.0228.v1

3.3. Linear Discriminant Analysis (LDA)

Employing LDA, we explored the accuracy of diagnosis classification based on different connectivity measures. As seen in Table 6, all methods are suitable for classification purposes (precision of at least 80%), although the best results were obtained for the LDA of full functional connectivity matrices. An illustration of the results is given in Figure 4 where the ROC-curves are presented.

Table 6. Classification accuracy of different connectivity features.

#	Feature vector	Accuracy (Mean±SD)	Sensitivity	Specificity	Precision
1	Full FC matrices	0.9376±0.0106	85%	98%	97%
2	FC matrices with significant connections	0.9146±0.0187	86%	96%	94%
3	Clustering coefficient	0.8424±0.0271	89%	79%	81%
4	Node strength	0.8457±0.0246	87%	82%	80%
5	Eigenvector centrality	0.8570±0.0256	83%	90%	87%

Gray line highlights the unsuitable feature for classification.

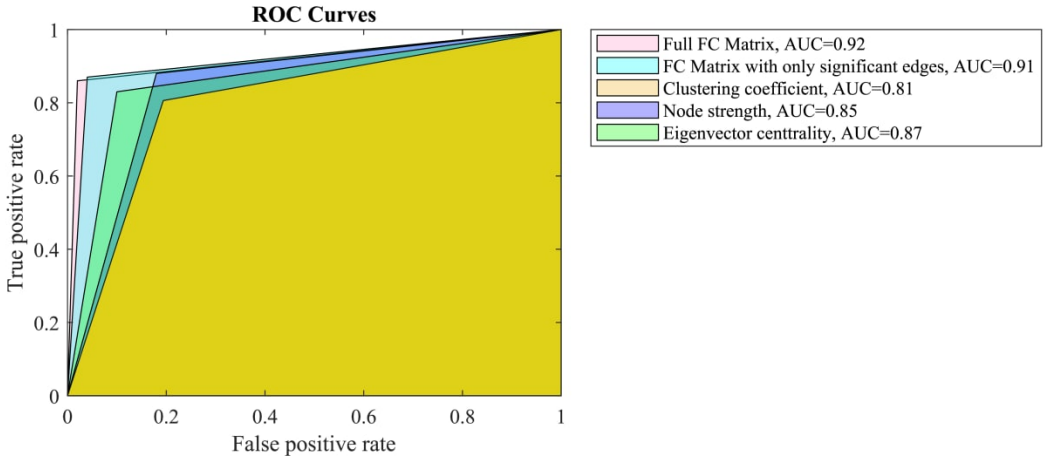

Figure 4. Receiver operating characteristic for the LDA classifiers for different feature vectors, AUC = Area under curve.

4. Discussion

The results of the current study point to significant differences in FC between a number of brain regions in depressed patients as compared to healthy controls. The most prominent changes were found in within-region as well as between-region connectivity of occipital lobe areas such as precuneus (PreCu), cuneus (Cu), superior occipital gyrus (SOG), lingual gyrus (LG), fusiform gyrus (FG), cerebellum, along with limbic structures including the hippocampus (Hipp) and cingulate gyrus.

The most significantly different connection was the one between the left and right PreCu. The function of the precuneus during rest is traditionally linked to the default mode network (DMN), which is responsible for internally oriented attention and self-reference (43). In this context, the current finding of changed connectivity within the PreCu is not surprising and it is in line with most resting-state studies of depression where the DMN, as well as its subregions, is found to be hyperactivated and hyperconnected (44, 45). This is usually linked to the clinical features of depression as a state of increased internalization (including ruminations) (46).

We found no significant difference in the global (network-wide averaged) eigenvector centrality, node strength, and clustering coefficient measures between the control and MDD groups. Thus, in terms of global network topology, the characteristic functional networks do not differ between the groups under consideration. The main differences are observed at the local level, as indicated by the significant clusters in the network measure distributions (see Tables 3-5).

 doi:10.20944/preprints202209.0228.v1

The first two positive clusters (Control>MDD) in the network measure distributions, in which eigenvector centrality, node strength, and clustering coefficient are higher in the control group, include bilateral lingual, superior, and middle occipital gyri and cerebellar (vermis). In terms of the network measures, a higher local clustering coefficient means that short-range (local) connections prevail over long-range (global) ones in these brain areas in the control group, and network clusters are formed there. A higher eigenvector centrality and node strength in the same nodes in the control group corresponds to a stronger integration of emerging clusters in the network and stronger connections of these nodes (hubs) with other large hubs. The remaining three positive clusters include the cingulate and thalamic nodes as well as the inferior frontal gyrus and are characterized by increased eigenvector centrality and node strength (only for the 3rd and 4th clusters) in the control group. This indicates that these nodes form larger and more strongly integrated into the network hubs compared to the MDD group. These conclusions are also supported qualitatively by Fig. 2.

Of note, all considered measures pointed to the role of the left LG as a major hub in the occipital cluster, with a number of connections demonstrating a significant difference in depressed as compared to healthy individuals. In accordance with these results, depression has been linked to impaired static and dynamic FC of the LG. The role of the left LG in depression has been reported in a most recent functional connectivity study assessing the effect of childhood trauma (47). The authors report that the FC changes of the left LG were not affected by the presence or absence of traumatic events, which may reflect a general vulnerability to depression. In support of this notion is the recent study of Wang et al. on electroconvulsive treatment of depression. The authors found changes in functional connectivity of the lingual gyrus to be persistent before as well as after the procedures (48).

The first negative cluster (MDD>Control), which is the same for all considered measures, includes the following brain areas: superior frontal gyrus (medial orbital), rectus gyrus, and medial and anterior orbital gyri. Thus, in the MDD group, more developed network clusters are formed near these nodes, while they are also more strongly integrated into the whole network, being large hubs (see also Fig. 3). The second negative cluster is unique for the eigenvector centrality measure and includes thalamic nodes. Note that a significantly large number of positive clusters in comparing the control and MDD groups is a characteristic feature of the functional network.

The most important to the clinical reality finding of the current study was derived from the linear discriminant analysis. It demonstrated that the clustering coefficient was the most ineffective measure while the full connectivity matrices, as well as those with only the significant connections identified in advance, were the most precise in differentiating between depression and health. These measures reached precision levels of 97% and 94%, respectively. Thus, the connectivity matrices outperformed the network-specific features of node strength and node centrality. We can speculate that in order to demonstrate a meaningful diagnostic value, the resting-state connectivity feature of depression should be considered as a whole and not reduced to separate network measures.

Earlier connectivity-based classification studies focused on specific regions or networks, some of them reaching very good accuracy levels of around 90% (49). Later, whole-brain connectivity analysis was favored, and the prediction levels reached 94% (50). Some of the most recent studies adopt a fusion strategy using different connectivity features (intrinsic, dynamic FC, effective connectivity) that could distinguish between MDD and controls with an accuracy of 90.91% and an AUC of 0.895 (51). In this regard, our study yielded one of the highest performances of the classifier based on whole-brain functional connectivity analysis.

5. Limitations

This study has several limitations that must be admitted. First, the sample size is relatively small, although comparable to other single-site studies. Second, the patient group is heterogeneous in terms of diagnosis (major depressive and bipolar disorder) and this may have influenced the results since both common and distinct activity and connectivity patterns have been demonstrated (52, 53). However, we have studied dysfunctional connectivity as a state dependent measure in major depressive episode. Unlike the trait (or state-independent indicators), clinical features as well as the underlying functional networks impairment on the level of the episode or the syndrome more or less shared between BAD and MDD. Third, the fact that all patients have been on stable antidepressant medication prior to inclusion might have contributed as well to our findings. Future research should address those limitations by increasing the number of subjects, exploring the two types of depression separately, and including samples of non-medicated patients.

6. Conclusion

In the recent decade, there is a major paradigm shift toward the network-connectivity-driven classification of mental disorders (54). Our work contributes to this field by providing insights into impairment of resting-state network functional connectivity hubs, including the lingual gyrus, demonstrating potential in patients with a major depressive episode when compared with healthy controls. Further integration of those results with structural and diagnostic task-related functional MRI on the level of multivariate analysis may outline new approaches and criteria to the definition of mental disorders (55, 56).

Funding: This research received no external funding

Institutional Review Board Statement: The study was conducted in accordance with the Declaration of Helsinki and approved by Ethics Committee of Medical University in Plovdiv (2/19.04.2018).

Informed Consent Statement: Informed consent was obtained from all subjects involved in the study.

Data Availability: All data is available from the authors upon reasonable request.

Conflicts of Interest: The authors declare no conflict of interest.

References

1. Reddy MS. Depression: the disorder and the burden. Indian J Psychol Med. 2010 Jan;32(1):1-2. doi: 10.4103/0253-7176.70510. PMID: 21799550; PMCID: PMC3137804.
2. Chen Z, Xia M, Zhao Y, Kuang W, Jia Z, Gong Q. Characteristics of Intrinsic Brain Functional Connectivity Alterations in Major Depressive Disorder Patients With Suicide Behavior. J Magn Reson Imaging. 2021 Dec;54(6):1867-1875. doi: 10.1002/jmri.27784. Epub 2021 Jun 16. PMID: 34137101.
3. I.H. Gotlib, J. Joormann, Cognition and depression: current status and future directions, Annu. Rev. Clin. Psychol., 6 (2010), pp. 285-312
4. Nierenberg AA, Husain MM, Trivedi MH, Fava M, Warden D, Wisniewski SR, Miyahara S, Rush AJ, Psychol Med. 2010 Jan; 40(1):41-50.
5. Liu J, Fan Y, Ling-Li Zeng, Liu B, Ju Y, Wang M, Dong Q, Lu X, Sun J, Zhang L, Guo H, Futao Zhao, Weihui Li, Zhang L, Li Z, Liao M, Zhang Y, Hu D, Li L. The neuroprogressive nature of major depressive disorder: evidence from an intrinsic connectome analysis. Transl Psychiatry. 2021 Feb 4;11(1):102. doi: 10.1038/s41398-021-01227-8. PMID: 33542206; PMCID: PMC7862649.
6. Biswal B, Yetkin FZ, Haughton VM, Hyde JS. Functional connectivity in the motor cortex of resting human brain using echo-planar MRI. Magn Reson Med. 1995;34(4):537-541. doi:10.1002/mrm.1910340409
7. Khramov A. E. et al. Functional networks of the brain: from connectivity restoration to dynamic integration. Physics-Uspekhi. 2021; 64(6):584. doi: 10.3367/UFNe.2020.06.038807
8. Drevets WC, Price JL, Furey ML. Brain structural and functional abnormalities in mood disorders: implications for neurocircuitry models of depression. Brain Struct Funct. 2008;213(1-2):93-118. doi:10.1007/s00429-008-0189-x
9. Rosazza, C., Minati, L. Resting-state brain networks: literature review and clinical applications. Neurol Sci 32, 773–785 (2011). doi:10.1007/s10072-011-0636-y
10. Dutta A, McKie S, Deakin JF. Resting state networks in major depressive disorder [published correction appears in Psychiatry Res. 2015 Dec 30;234(3):392-7]. Psychiatry Res. 2014;224(3):139-151. doi:10.1016/j.pscychresns.2014.10.003

11. Zhang J, Cui H, Yang H, et al. Dynamic changes of large-scale resting-state functional networks in major depressive disorder. Prog Neuropsychopharmacol Biol Psychiatry. 2021;111:110369. doi:10.1016/j.pnpbp.2021.110369
12. Ebneabbasi A, Mahdipour M, Nejati V, et al. Emotion processing and regulation in major depressive disorder: A 7T resting-state fMRI study. Hum Brain Mapp. 2021;42(3):797-810. doi:10.1002/hbm.2526313
13. Pizzagalli DA. Frontocingulate dysfunction in depression: toward biomarkers of treatment response. Neuropsychopharmacology. 2011;36(1):183-206. doi:10.1038/npp.2010.166
14. Yao Z, Fu Y, Wu J, Zhang W, Yu Y, Zhang Z, Wu X, Wang Y, Hu B. Morphological changes in subregions of hippocampus and amygdala in major depressive disorder patients. Brain Imaging Behav. 2020 Jun;14(3):653-667. doi: 10.1007/s11682-018-0003-1. PMID: 30519998; PMCID: PMC6551316.
15. Schindler S, Schmidt L, Stroske M, Storch M, Anwander A, Trampel R, Strauß M, Hegerl U, Geyer S, Schönknecht P. Hypothalamus enlargement in mood disorders. Acta Psychiatr Scand. 2019 Jan;139(1):56-67. doi: 10.1111/acps.12958. Epub 2018 Sep 19. PMID: 30229855.
16. W.C. Drevets. Neuroimaging studies of mood disorders. Biol. Psychiatry, 48 (2000), pp. 813-829. doi:10.1016/S0006-3223(00)01020-9
17. P.C. Mulders, P.F. van Eijndhoven, A.H. Schene, C.F. Beckmann, I. Tendolkar, Resting-state functional connectivity in major depressive disorder: a review,Neurosci. Biobehav. Rev. (2015), doi:10.1016/j.neubiorev.2015.07.014
18. R.H. Kaiser, J.R. Andrews-Hanna, T.D. Wager, D.A. Pizzagalli, Large-Scale network dysfunction in major depressive disorder, JAMA Psychiatry (2015), doi:10.1001/jamapsychiatry.2015.0071
19. J.P. Hamilton, G.H. Glover, E. Bagarinao, C. Chang, S. Mackey, M.D. Sacchet, I.H. Gotlib, Effects of salience-network-node neurofeedback training on affective biases in major depressive disorder, Psychiatry Res. Neuroimaging. (2016), doi:10.1016/j.pscychresns.2016.01.016
20. Saris IMJ, Penninx BWJH, Dinga R, van Tol MJ, Veltman DJ, van der Wee NJA, Aghajani M. Default Mode Network Connectivity and Social Dysfunction in Major Depressive Disorder. Sci Rep. 2020 Jan 13;10(1):194. doi: 10.1038/s41598-019-57033-2. PMID: 31932627; PMCID: PMC6957534.
21. Fateh AA, Long Z, Duan X, Cui Q, Pang Y, Farooq MU, Nan X, Chen Y, Sheng W, Tang Q, Chen H. Hippocampal functional connectivity-based discrimination between bipolar and major depressive disorders. Psychiatry Res Neuroimaging. 2019 Feb 28;284:53-60. doi: 10.1016/j.pscychresns.2019.01.004. Epub 2019 Jan 12. PMID: 30684896.
22. Luo L, Wu H, Xu J, et al. Abnormal large-scale resting-state functional networks in drug-free major depressive disorder. Brain Imaging Behav. 2021;15(1):96-106. doi:10.1007/s11682-019-00236-y
23. Yang Y, Zhong N, Imamura K, et al. Task and Resting-State fMRI Reveal Altered Salience Responses to Positive Stimuli in Patients with Major Depressive Disorder. PLoS One. 2016;11(5):e0155092. Published 2016 May 18. doi:10.1371/journal.pone.0155092
24. Liang S, Deng W, Li X, et al. Biotypes of major depressive disorder: Neuroimaging evidence from resting-state default mode network patterns. Neuroimage Clin. 2020;28:102514. doi:10.1016/j.nicl.2020.102514
25. Sen B, Mueller B, Klimes-Dougan B, Cullen K, Parhi KK. Classification of Major Depressive Disorder from Resting-State fMRI. Annu Int Conf IEEE Eng Med Biol Soc. 2019;2019:3511-3514. doi:10.1109/EMBC.2019.8856453
26. Zhu X, Yuan F, Zhou G, et al. Cross-network interaction for diagnosis of major depressive disorder based on resting state functional connectivity. Brain Imaging Behav. 2021;15(3):1279-1289. doi:10.1007/s11682-020-00326-2
27. Alexopoulos GS, Hoptman MJ, Kanellopoulos D, Murphy CF, Lim KO, Gunning FM. Functional connectivity in the cognitive control network and the default mode network in late-life depression. J Affect Disord. 2012;139(1):56-65. doi:10.1016/j.jad.2011.12.002
28. Zeng LL, Shen H, Liu L, et al. Identifying major depression using whole-brain functional connectivity: a multivariate pattern analysis. Brain. 2012;135(Pt 5):1498-1507. doi:10.1093/brain/aws059
29. Sheehan DV, Lecrubier Y, Sheehan KH, et al. The Mini-International Neuropsychiatric Interview (M.I.N.I.): the development and validation of a structured diagnostic psychiatric interview for DSM-IV and ICD-10. J Clin Psychiatry. 1998;59 Suppl 20:22-57.
30. Montgomery SA, Asberg M. A new depression scale designed to be sensitive to change. Br J Psychiatry. 1979;134:382-389. doi:10.1192/bjp.134.4.382
31. Rolls ET, Huang CC, Lin CP, Feng J, Joliot M. Automated anatomical labelling atlas 3. Neuroimage. 2020;206:116189. doi:10.1016/j.neuroimage.2019.116189
32. Stanley ML, Moussa MN, Paolini BM, Lyday RG, Burdette JH, Laurienti PJ. Defining nodes in complex brain networks. Front Comput Neurosci. 2013;7:169. Published 2013 Nov 22. doi:10.3389/fncom.2013.00169
33. Bastos AM, Schoffelen JM. A Tutorial Review of Functional Connectivity Analysis Methods and Their Interpretational Pitfalls. Front Syst Neurosci. 2016 Jan 8;9:175. doi: 10.3389/fnsys.2015.00175. PMID: 26778976; PMCID: PMC4705224.
34. Rubinov M, Sporns O. Weight-conserving characterization of complex functional brain networks. Neuroimage. 2011;56(4):2068-2079. doi:10.1016/j.neuroimage.2011.03.069
35. Bassett DS, Sporns O. Network neuroscience. Nat Neurosci. 2017;20(3):353-364. doi: 10.1038/nn.4502.
36. Costantini G, Perugini M. Generalization of clustering coefficients to signed correlation networks. PLoS One. 2014;9(2):e88669. Published 2014 Feb 21. doi:10.1371/journal.pone.008866937.

37. Newman, Mark EJ. "The mathematics of networks." The new palgrave encyclopedia of economics 2.2008 (2008): 1-12.
38. Genovese CR, Lazar NA, Nichols T. Thresholding of statistical maps in functional neuroimaging using the false discovery rate. Neuroimage. 2002;15(4):870-878. doi:10.1006/nimg.2001.1037
39. Zalesky A., Fornito A., Bullmore E. T. Network-based statistic: identifying differences in brain networks. Neuroimage. 2010;53(4):1197-1207.
40. Maris E, Oostenveld R. Nonparametric statistical testing of EEG- and MEG-data. J Neurosci Methods. 2007;164(1):177-190. doi:10.1016/j.jneumeth.2007.03.024
41. Xia M, Wang J, He Y. BrainNet Viewer: a network visualization tool for human brain connectomics. PLoS One. 2013;8(7):e68910. doi:10.1371/journal.pone.006891042.
42. Fernandes BS, Karmakar C, Tamouza R, et al. Precision psychiatry with immunological and cognitive biomarkers: a multi-domain prediction for the diagnosis of bipolar disorder or schizophrenia using machine learning. Transl Psychiatry. 2020;10(1):162. Published 2020 May 24. doi:10.1038/s41398-020-0836-4
43. Sheline, Yvette I., Deanna M. Barch, Joseph L. Price, Melissa M. Rundle, S. Neil Vaishnavi, Abraham Z. Snyder, Mark A. Mintun, Suzhi Wang, Rebecca S. Coalson, and Marcus E. Raichle. 2009."The default mode network and self-referential processes in depression." Proceedings of the National Academy of Sciences 106 (6):1942-1947.
44. Brakowski, J., S. Spinelli, N. Dorig, O. G. Bosch, A. Manoliu, M. G. Holtforth, and E. Seifritz. 2017. "Resting state brain network function in major depression - Depression symptomatology, antidepressant treatment effects, future research." J Psychiatr Res 92:147-159. doi: 10.1016/j.jpsychires.2017.04.007.
45. Sambataro, F., N. D. Wolf, M. Pennuto, N. Vasic, and R. C. Wolf. 2014. "Revisiting default mode network function in major depression: evidence for disrupted subsystem connectivity." Psychol Med 44 (10):2041-51. doi: 10.1017/s0033291713002596.
46. Whitfield-Gabrieli, S., and J. M. Ford. 2012. "Default mode network activity and connectivity in psychopathology." Annu Rev Clin Psychol 8:49-76. doi: 10.1146/annurev-clinpsy-032511-143049.
47. Luo, Q., J. Chen, Y. Li, Z. Wu, X. Lin, J. Yao, H. Yu, H. Peng, and H. Wu. 2022. "Altered regional brain activity and functional connectivity patterns in major depressive disorder: A function of childhood trauma or diagnosis?" J Psychiatr Res 147:237-247. doi: 10.1016/j.jpsychires.2022.01.038.
48. Wang J, Ji Y, Li X, He Z, Wei Q, Bai T, Tian Y, Wang K. Improved and residual functional abnormalities in major depressive disorder after electroconvulsive therapy. Prog Neuropsychopharmacol Biol Psychiatry. 2020 Jun 8;100:109888. doi: 10.1016/j.pnpbp.2020.109888. Epub 2020 Feb 17. PMID: 32061788.
49. Zeng, L. L., H. Shen, L. Liu, and D. Hu. 2014. "Unsupervised classification of major depression using functional connectivity MRI." Hum Brain Mapp 35 (4):1630-41. doi: 10.1002/hbm.22278.
50. Zeng, L. L., H. Shen, L. Liu, L. Wang, B. Li, P. Fang, Z. Zhou, Y. Li, and D. Hu. 2012. "Identifying major depression using whole-brain functional connectivity: a multivariate pattern analysis." Brain 135 (Pt 5):1498-507. doi: 10.1093/brain/aws059.
51. Li, Y., X. Dai, H. Wu, and L. Wang. 2021. "Establishment of Effective Biomarkers for Depression Diagnosis With Fusion of Multiple Resting-State Connectivity Measures." Front Neurosci 15:729958. doi: 10.3389/fnins.2021.729958.
52. Delvecchio, G., P. Fossati, P. Boyer, P. Brambilla, P. Falkai, O. Gruber, J. Hietala, S. M. Lawrie, J. L. Martinot, A. M. McIntosh, E. Meisenzahl, and S. Frangou. 2012. "Common and distinct neural correlates of emotional processing in Bipolar Disorder and Major Depressive Disorder: a voxel-based meta-analysis of functional magnetic resonance imaging studies." Eur Neuropsychopharmacol 22 (2):100-13. doi: 10.1016/j.euroneuro.2011.07.003.
53. Cardoso de Almeida, J. R., and M. L. Phillips. 2013. "Distinguishing between unipolar depression and bipolar depression: current and future clinical and neuroimaging perspectives." Biol Psychiatry 73 (2):111-8. doi: 10.1016/j.biopsych.2012.06.010.
54. Schmidt A, Diwadkar VA, Smieskova R, Harrisberger F, Lang UE, McGuire P, Fusar-Poli P, Borgwardt S. Approaching a network connectivity-driven classification of the psychosis continuum: a selective review and suggestions for future research. Front Hum Neurosci. 2015 Jan 13;8:1047. doi: 10.3389/fnhum.2014.01047. PMID: 25628553; PMCID: PMC4292722.
55. Paunova R, Kandilarova S, Todeva-Radneva A, Latypova A, Kherif F, Stoyanov D. Application of Mass Multivariate Analysis on Neuroimaging Data Sets for Precision Diagnostics of Depression. Diagnostics (Basel). 2022;12(2):469. Published 2022 Feb 12. doi:10.3390/diagnostics12020469
56. Simeonova, D., Paunova, R., Stoyanova, K., Todeva-Radneva, A., Kandilarova, S., & Stoyanov, D. (2022). Functional MRI Correlates of Stroop N-Back Test Underpin the Diagnosis of Major Depression. *Journal of Integrative Neuroscience*, *21*(4), 113. doi: 10.31083/j.jin2104113